DOI: 10.1002/cphc.200600283

Control of Molecular Fragmentation Using Binary Phase-Shaped Femtosecond Laser Pulses

Vadim V. Lozovoy, Tissa C. Gunaratne, Janelle C. Shane, and Marcos Dantus*[a]

The quest for laser control of chemical reactions has progressed along different paths that although significant, have not provided a solid scientific understanding. Beyond the first demonstrations, projects have explored what level of control may be possible using learning algorithms that are capable of testing a very wide range of phase- and amplitude-shaped pulses.[1] A different approach has been to narrow down the types of pulses used to achieve robust control that can be applied for molecular identification.[2,3] Here we present a systematic study that can be used to address some of the fundamental scientific questions regarding the observed fragmentation control resulting from the intense laser molecule interactions. The data consist of results obtained from 256 differently shaped femtosecond pulses on *ortho*-nitrotoluene (*o*-NT), that were repeated ten times for statistical analysis. We present some of the observed trends from this set of measurements. We consider this analysis to be useful and revealing; however, it is still far from providing a satisfactory explanation for the observations. We hope that making these data available will stimulate additional scientific discussion.

Laser excitation of nitrobenzene and isomers of nitrotoluenes with nanosecond laser pulses[4] produces a large number of small fragments whose presence is attributed to a mechanism involving dissociation followed by ionization, a mechanism also known as ladder switching.[5] For femtosecond pulses, the dissociation process is overridden by a faster multiphoton ionization process, leading to the observation of the molecular ion as well as other heavier fragments.[6] This observation is believed to proceed through a mechanism where multiphoton ionization (ladder climbing) is followed by dissociation through a systematic breakdown of the initially formed molecular ion.

A Ti:sapphire oscillator and regenerative amplifier laser was used capable of producing transform-limited (TL) 35 fs pulses, 0.8 mJ per pulse at 1 kHz. Phase distortions at the sample are corrected with a 128 pixel spatial light modulator located before the amplifier, using the multiphoton intrapulse interference phase scan (MIIPS™) technique developed in our laboratory.[7] The beam is attenuated to 170 μJ per pulse and focused with a 50 mm lens into the vacuum chamber of a time-of-flight mass spectrometer. *Ortho*-nitrotoluene (Aldrich, 99%) was used as received and introduced to the chamber to maintain a background pressure of 1×10^{-5} Torr, under fast flow conditions. Eight-bit binary phase functions, with spectral phase values of 0 and π (logical 0 and 1), were applied.[8] The first and last bits were placed on the weak spectral wings and the six central bits were evenly binned with 10 SLM pixels per bit. Mass spectra were collected, averaging 256 laser pulses per phase function. Experiments on the entire set of eight-bit phase functions were repeated 10 times to determine the statistical significance of each result. Relative yields were calculated by dividing the intensity of a particular ion by the integrated intensity of all observed fragments in the mass spectrum obtained by a given shaped pulse.

The mass spectrum of *o*-NT obtained with TL pulses (vertical bars) is shown in Figure 1. The dark and light grey shaded areas terminate at the maximum and minimum relative yields observed for each fragment, respectively. Figure 1 summarizes the results from all the phase functions evaluated, and shows the maximum extent to which the relative yield of each fragment can be manipulated. The relative yields of heavier ions are maximized by TL pulses, as evidenced by the bar heights matching that of the dark grey shaded region. The appearance energies for some of the fragment ions are included. Highly modulated pulses maximize the relative yields of the lighter fragments. For example, the binary shaped pulse (01010110) reduces the line with $m/z=120$, corresponding to $C_7H_6NO^+$, to the noise level.

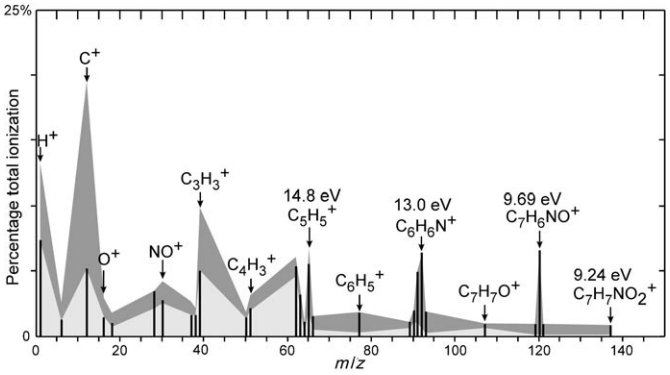

Figure 1. Percentage of total ionization of *o*-NT. The bars represent the data obtained with TL pulses while dark and light grey areas represent the absolute maximum and minimum yields for each fragment ion. The shaded regions summarize results obtained using the entire set of 256 binary phase functions. Selected fragment ions are labeled together with their appearance energy.

Changes in relative yields for each fragment ion can best be visualized by a spider plot, as shown in Figure 2. Each fragment ion is represented by a vector with origin at the center and with a length equivalent to its relative yield (note logarithmic scale). The mass spectrum resulting from TL pulses is used to normalize the intensities of the fragment ions. The resulting relative yields obtained for a particular shaped pulse are connected to create a polygon, making it easy to see the overall trend for a given binary shaped laser pulse. The binary phase

[a] *Dr. V. V. Lozovoy, Dr. T. C. Gunaratne, J. C. Shane, Prof. M. Dantus*
Department of Chemistry, Michigan State University
East Lansing MI 4882 (USA)
Fax: (+11) 517-353-1793
E-mail: dantus@msu.edu

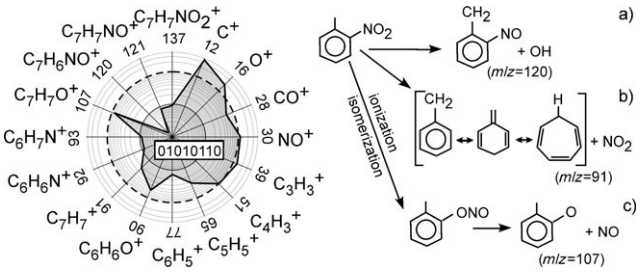

Figure 2. Spider plot representation of the changes in the relative yields (logarithmic scale) of a number of fragment ions as a result of binary phase shaping. Results for TL pulses are indicated by the dashed circle, where all fragments are assigned a relative yield of unity. The solid line represents yields for the eight-bit phase function that provided the strongest suppression of the ion with $m/z = 120$, which is most abundant at TL excitation. Possible reactions responsible for the yield of heavy fragments: a) *ortho* effect or OH elimination yields $C_7H_6NO^+$ with $m/z = 120$; b) NO_2 elimination gives alternative structures of the tropylium ion $C_7H_7^+$ with $m/z = 91$; c) isomerization of molecular cation followed by NO loss yields $C_7H_7O^+$ with $m/z = 107$.

shown in Figure 2 is (01010110), which was observed to give the greatest decrease in the relative yield of $C_7H_6NO^+$. A general trend becomes apparent. Pulse shaping suppresses the relative yield of heavy ions ($m/z \geq 65$) and enhances the relative yield of lighter ions ($m/z < 65$). TL pulses maximize the yield of larger fragments, those with an aromatic ring structure. Cleaving the benzene ring requires longer pulses, produced by the more complex binary phase functions. The fragmentation pathways giving rise to the larger fragment ions include hydrogen abstraction "the *ortho*-effect" (Figure 2a) which can take place in ionized or neutral molecules; loss of NO_2 and formation of tropylium ion (Figure 2b); and sequential ionization, isomerization and dissociation (Figure 2c) which involves isomerization of the nitro group[9] followed by NO dissociation.

In Figure 3, we display the relative yield of selected ions (sorted according to total yield of all ions) obtained for all eight-bit phase functions evaluated. The yield of $C_7H_6NO^+$ (OH loss) is maximized by TL pluses and suppressed by a factor of one hundred for shaped pulses from a small set of binary phase functions. We also note that $C_7H_7O^+$ and NO^+ [the isomerization pathway (Figure 2c)] stay relatively constant and under closer inspection appear uncorrelated, at least within the experimental noise level. The absence of correlation between C_7H_7O and NO indicates that the observed NO ion is not a simple product of decay after isomerization. In this case, the charge probably stays in the aromatic fragment and NO is therefore neutral and does not appear in the spectrum. Yields of smaller fragments, including the smallest and most sensitive C^+, increase when the pulse is shaped.

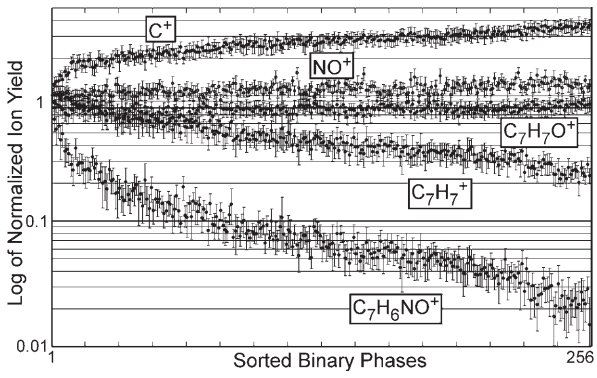

Figure 3. Relative yield observed for different fragment ions sorted according to the integrated mass spectrum intensity. For each binary phase we give the average intensity, normalized on the value obtained for TL pulses, along with the standard deviation.

The most important observation from Figure 3 is that once sorted for total ion yield, the results plotted for individual ion yields are monotonic. Because there is a direct relationship between total ion yield and the total intensity of a pulse's second harmonic (SHG) spectrum, individual ion yields are also monotonic with respect to total SHG intensity. This means that for any binary shaped pulse, if we know the total ion yield (or total SHG intensity) we can predict the individual fragment ion yields. The data show clear global maxima and minima that correlate with total ion yield. The same relationship is observed for chirp and sinusoidal phase functions.[10] In other words, we have not found evidence for "magic" pulses that can cleanly break a chemical bond selectively. The enhanced ionization model[11] may be used to explain the controllability observed among different pathways. Enhanced ionization occurs when bonds undergo stretching and requires time for atomic displacement; 35 fs TL pulses are too fast and minimize fragmentation, but binary shaped pulses create highly modulated and long pulses.

Binary phase shaping provides a very robust platform for designing applications for three reasons. First, from a mathematical point of view, binary phases allow us to borrow results from number theory to design phases and estimate the level of controllability.[12] Second, from a technical point of view, binary phases can be easily implemented by a shaper with only two retardances $(0,\pi)$; they are also very easy to reproduce accurately. Third, and most important, there is a physical motivation for exploring binary spectral phase functions. The nonlinear optical response of the sample depends on multiphoton intrapulse interference.[8,13] Interference between quantum mechanical pathways depends on their relative phase. Binary phase functions give us the most efficient means of controlling the phase imparted on each pathway to achieve constructive or destructive interference. As illustrated here using a spider plot representation, eight-bit binary phase functions affect fragmentation by more than two orders of magnitudes. For these three reasons binary phase shaping is ideally suited for developing robust methods for molecular recognition that would be valuable for analytical chemistry.[3]

Acknowledgements

We acknowledge the contributions of Michael J. Kangas during the data collection stage of this study. This research was supported in part by the National Science Foundation and by an STTR grant to BioPhotonic Solutions Inc from the US Army Research Office (the content of the information does not necessarily reflect

the position or the policy of the Government; no official endorsement should be inferred).

Keywords: femtochemistry · laser chemistry · mass spectrometry · pulse shaping

[1] A. Assion, T. Baumart, M. Bergt, T. Brixner, B. Kiefer, V. Sayfried, M. Strehle, G. Gerber, *Science* **1998**, *282*, 919 – 922; R. J. Levis, G. M. Menkir, H. Rabitz, *Science* **2001**, *292*, 709 – 713; B. J. Pearson, J. L. White, T. C. Weinacht, P. H. Bucksbaum, *Phys. Rev. A* **2001**, *63*, 063412.

[2] I. Pastirk, M. Kangas, M. Dantus, *J. Phys. Chem. A* **2005**, *109*, 2413 – 2416.

[3] J. M. Dela Cruz, V. V. Lozovoy, M. Dantus, *J. Phys. Chem. A* **2005**, *109*, 8447 – 8450.

[4] C. Kosmidis, A. Marshall, A. Clark, R. M. Deas, K. W. D. Ledingham, R. P. Singhal, *Rapid Commun. Mass Spectrom.* **1994**, *8*, 607 – 614; C. Kosmidis, K. W. D. Ledingham, H. S. Killic, T. McCanny, R. P. Singhal, A. J. Langley, W. Shaikh, *J. Phys. Chem. A* **1997**, *101*, 2264 – 2270.

[5] L. Zandee, R. B. Bernstein, *J. Chem. Phys.* **1979**, *71*, 1359 – 1371; D. M. Lubman, R. Naaman, R. N. Zare, *J. Chem. Phys.* **1980**, *72*, 3034 – 3040; J. J. Yang, D. A. Gobeli, M. A. Elsayed, *J. Phys. Chem.* **1985**, *89*, 3426 – 3429; S. M. Hankin, A. D. Tasker, L. Robson, K. W. D. Ledingham, X. Fang, P. McKenna, T. McCanny, R. P. Singhal, C. Kosmidis, P. Tzallas, D. A. Jaroszynski, R. Jones, R. C. Issac, S. Jamison, *Rapid Commun. Mass Spectrom.* **2002**, *16*, 111 – 116.

[6] C. Weickhardt, K. Tonnies, *Rapid Commun. Mass Spectrom.* **2002**, *16*, 422 – 446.

[7] V. V. Lozovoy, I. Pastirk, M. Dantus, *Opt. Lett.* **2004**, *29*, 775 – 777; B. W. Xu, J. M. Gunn, J. M. Dela Cruz, V. V. Lozovoy, M. Dantus, *J. Opt. Soc., Am. B* **2006**, *23*, 750 – 759.

[8] M. Comstock, V. V. Lozovoy, I. Pastirk, M. Dantus, *Opt. Express* **2004**, *12*, 1061 – 1066.

[9] T. H. Osterheld, T. Baer, J. I. Brauman, *J. Am. Chem. Soc.* **1993**, *115*, 6284 – 6289.

[10] unpublished results.

[11] M. Ivanov, T. Seideman, P. Corkum, F. Ilkov, P. Dietrich, *Phys. Rev. A* **1996**, *54*, 1541 – 1550; R. Itakura, K. Yamanouchi, T. Tanabe, T. Okamoto, F. Kannari, *J. Chem. Phys.* **2003**, *119*, 4179 – 4186; D. Cardoza, F. Langhojer, C. Trallero-Herrero, O. L. A. Monti, T. Weinacht, *Phys. Rev. A* **2004**, *70*, Art. No. 053406; D. Cardoza, M. Baertschy, T. Weinacht, *Chem. Phys. Lett.* **2005**, *411*, 311 – 315; F. Langhojer, D. Cardoza, M. Baertschy, T. Weinacht, *J. Chem. Phys.* **2005**, *122*, Art. No. 014102.

[12] V. V. Lozovoy, B. Xu, J. C. Shane, M. Dantus, *Phys. Rev. A.* **2006**, unpublished results.

[13] K. A. Walowicz, I. Pastirk, V. V. Lozovoy, M. Dantus, *J. Phys. Chem. A.* **2002**, *106*, 9369 – 9373; V. V. Lozovoy, I. Pastirk, K. A. Walowicz, M. Dantus, *J. Chem. Phys.* **2003**, *118*, 3187 – 3196; V. V. Lozovoy, M. Dantus, *ChemPhysChem* **2005**, *6*, 1970 – 2000.

Received: May 5, 2006
Revised: September 14, 2006
Published online on October 30, 2006

